

C₁ AND C₂ FLUORINATED HYDROCARBON EFFECTS ON THE EXTINCTION CHARACTERISTICS OF METHANE VS. AIR COUNTERFLOW DIFFUSION FLAMES

Michael A. Tanoff*, Richard R. Dobbins, Mitchell D. Smooke
Department of Mechanical Engineering, Yale University
P.O. Box 208284
New Haven, Connecticut, U.S.A. 06520-8284

Donald R. Burgess, Jr., Michael R. Zachariah, Wing Tsang
Chemical Science and Technology Laboratory
National Institute of Standards and Technology
Gaithersburg, Maryland, U.S.A. 20899-0001

Phillip R. Westmoreland
Department of Chemical Engineering, University of Massachusetts
Amherst, Massachusetts, U.S.A. 01009-9110

ABSTRACT

Detailed numerical calculations are compared against available experiments and are used to investigate the flame suppression and extinction properties of a variety of fluorinated hydrocarbon candidates selected for halon 1301 and halon 1211 replacement. The air stream in a methane vs. air counterflow diffusion flame is doped with varying amounts of CH₃F, CH₂F₂, CHF₃, CF₄, CHF₂-CF₃ and CH₂F-CF₃, as well as the diluents N₂ and CO₂, and their effect on the strain rate required for flame extinction is monitored. The chemical model is based on a recently developed set of thermochemical and chemical kinetic data for the C₁ and C₂ fluorinated hydrocarbons.

Numerical results are in very good agreement with available experimental data for CF₄- and CHF₃-suppressed methane vs. air counterflow diffusion flames. Both computations and experiments show similar linear decreases in required extinction strain rate with molar per cent agent added to the oxidizer stream, thereby yielding the same effectiveness for suppressing flames. The model and associated chemical kinetic mechanism and thermodynamic data base predict moderately lower extinction strain rates throughout the entire range of suppressant addition level, and calculations with alternate sets of C/H/O kinetics are presented.

On a molar basis, the C₂ hydrofluorocarbons are more effective than their C₁ counterparts in causing methane vs. air counterflow flames to extinguish. However, on a mass basis, the inerts N₂ and CO₂ are comparable to or outperform *all* of the fluorinated species in extinguishing the methane vs. air counterflow flames. This important result may lessen the attractiveness of fluorocarbons and hydrofluorocarbons as replacements for halons 1301 and 1211 in certain applications.

The chemical activity of CHF₃ is shown to contribute towards flame suppression, particularly at higher concentrations. In contrast, the C₂ hydrofluorocarbons appear to provide very little net chemical contribution towards extinguishing the counterflow diffusion flames, and in fact, may contribute to slight flame enhancement in some cases. Additives which lead to CF₂O formation are more effective flame suppression agents than those whose chemistry tends to bypass this pathway, as the relatively stable CF₂O molecule prevents certain amounts of C, F and O atoms from participating in highly exothermic CO₂ and HF formation.

INTRODUCTION

Environmental problems associated with halon fire suppression agents are well publicized. In particular, production of the very effective brominated fire fighting agents, halon 1301 (CF₃Br) and halon 1211 (CF₂ClBr) — which have been used as chemical fire

* Corresponding author. tanoff@biomed.med.yale.edu; Phone: 203-432-4245;
Fax: 203-432-6775

extinguishers in ships, aircraft and computer sites — has been banned under international agreement since January 1, 1994 [1], due to the catalytically deleterious effect of the bromine atom on stratospheric ozone. Hydrochlorofluorocarbons (HCFCs) have a similar deleterious effect on the ozone layer, and their production is scheduled to be phased out by 2030.

Still, halons offer an attractive choice as agents for fire suppression applications because of their inhibiting flames with low concentrations, leaving no residue, and possessing a number of important physical properties — high level of stability, high liquid density, low boiling point, low corrosiveness and low toxicity — all at low cost [2]. The most promising replacements for suppression agents halon 1301 and halon 1211 seem to be fluorocarbons (FCs) and hydrofluorocarbons (HFCs).

Flame suppressing properties of FCs and HFCs have been investigated previously. Studies include numerical investigations of flame speeds, flame temperatures and species concentrations in freely propagating laminar flames [3], experimental and numerical studies of flame speeds in fluoromethane-suppressed premixed methane flames [4], a numerical study on the influence of Br-, I-, and F-containing inhibitors on premixed methane, methanol, ethane and ethylene flames [5], and experimental investigation of extinction and blowoff in counterflow and coflow diffusion flames burning various liquid fuels [6]. The former investigation [3] used a lean ($\phi = 0.65$) freely propagating laminar flame to study the flame suppression properties and chemical pathways of the fluoromethanes. It included the development of a fluorocarbon thermochemistry and kinetics data base which was the predecessor of the data base to be used in the present study.

More recently, the effectiveness of fluorinated suppression agents in extinguishing counterflow diffusion flames has been investigated. Fallon, Chelliah and Linteris [7] performed a combined experimental and numerical investigation on the effects of CHF_3 addition in extinguishing counterflow CO/H_2 vs. air flames. Papas, Fleming and Sheinson [8] used laser Doppler velocimetry to investigate the extinction conditions in CF_4 - and CHF_3 -suppressed methane vs. air and propane vs. air counterflow diffusion flames, and compared these results against the effectiveness of halon 1301 (CF_3Br).

In the present paper, we extend the application of a recently developed set of chemical kinetics [9] to investigate numerically the flame suppression and extinction characteristics of a wider set of fluorinated hydrocarbon agents, by doping the air stream in a methane vs. air counterflow diffusion flame with 0–8% (molar basis) of the hydrofluorocarbons CH_3F , CH_2F_2 , CHF_3 , $\text{CHF}_2\text{-CF}_3$ and $\text{CH}_2\text{F-CF}_3$, and the fluorocarbon CF_4 , as well as the “inerts” N_2 and CO_2 . Results for CF_4 and CHF_3 addition are compared directly to the aforementioned experiments [8]. We present the modeling approach, including the computational method and chemical mechanism, in the next section, after which the results are presented, and conclusions drawn.

MODEL

Computational Approach

We consider a laminar diffusion flame stabilized on the oxidizer side of the stagnation plane between two axisymmetric, counterflowing jets of finite separation. One jet contains the methane fuel and the other jet contains the air and any additive. The complete formulation of the mathematical model for solving the finite burner separation problem with plug flow boundary conditions is described in detail elsewhere [10,11].

Briefly, we begin with the elliptic form, in cylindrical coordinates, of the two-

dimensional equations describing the conservation of total mass, individual chemical species mass, momentum and energy for the reactive flow occurring between the two burners. In order to reduce the complexity of the problem, we seek a similarity solution of the form

$$\mathbf{u} = v(z), \mathbf{u} = rU(z), Y_k = Y_k(z), T = T(z), \quad (1)$$

in which r and z are the independent radial and axial coordinates; u and v are the radial and axial components of the flow velocity; Y_k is the mass fraction of the k th chemical species; and T is the temperature. If the expressions for u and u are substituted into the continuity and momentum equations, one finds that the axial pressure gradient and the reduced radial pressure gradient are, at most, functions of z alone. A consequence of this is that the reduced radial pressure gradient must be a constant, i.e.,

$$\frac{1}{r} \frac{\partial p}{\partial r} = J = \text{constant}, \quad (2)$$

in which p is the pressure. This result, coupled with the similarity transformations, reduces the governing equations to a nonlinear, two-point boundary value problem in the axial (z) direction along the stagnation point streamline. These equations are discretized with an adaptive finite difference algorithm and solved using Newton's method. The system is closed with an equation of state (in this case, the ideal gas law) and appropriate boundary conditions, for which plug flow is assumed for the velocity boundaries.

In order to determine the strain rate at extinction, we increase the velocity in the boundary condition of the air jet until the flame extinguishes. In order to do this efficiently, we employ the adaptive arclength continuation algorithm [10,12], which determines the sensitivity of the flame structure to the strain rate, alleviating the need to recalculate flame solutions completely for each new jet velocity. The discrete grid is adapted at *each* new strain rate, i.e., for each new flame, maintaining a preprescribed solution accuracy up to and including the extinction point. Rather than simply adding points at locations of high spatial activity, the entire grid is reevaluated for a given solution profile, thus maintaining a fairly constant number of grid points throughout the duration of the continuation calculation.

It is important to note that in the preceding mathematical formulation, the governing equations do not explicitly contain the strain rate, which we will denote as a . The magnitude of the reduced pressure gradient, J , is related to the strain of the flame due to the imposed flow. Thus, as J increases, so does the strain rate, and we could use J as a measure of a characteristic strain rate. However, a more commonly accepted measure of an effective strain rate is the maximum value of the oxidizer-side velocity gradient just prior to the flame [11]. We will use this measure of strain rate in the discussion that follows.

The model employs detailed chemical kinetics and transport properties, the development of which will be described shortly. The chemical production rates, binary diffusion coefficients, mixture viscosity and mixture thermal conductivity are evaluated using highly optimized transport and chemistry libraries [13]. The model includes thermal diffusion for light species, as well as heat losses due to radiation.

All calculations were performed on an IBM RS/6000-590 workstation. For a typical grid containing 130 discrete points (with 84 algebraic unknowns — temperature, velocity variables, pressure gradient eigenvalue, and 80 chemical species — at each point), each flame calculation, which includes convergence on the previous flame's grid and reconvergence on the adapted grid, required approximately 8.5 minutes of CPU time. Thus, a typical extinction calculation requiring 50–100 continuation steps required approximately 7–14 hours of CPU time.

Chemical Mechanism

We developed a comprehensive, detailed chemical kinetic mechanism for the reactions of C_1 and C_2 fluorinated hydrocarbon species in flames [9], which supersedes our earlier work on fluoromethane chemistry [3]. Existing fluorinated hydrocarbon thermochemistry and kinetics were compiled from the literature and evaluated. For species where no or incomplete thermochemistry was available, these data were calculated through application of BAC-MP4 formalism [14,15] for *ab initio* molecular orbital theory. Group additivity values were developed that were consistent with experimental and *ab initio* data. For reactions where no or limited kinetics was available, these data were estimated by analogy to hydrocarbon reactions, by using empirical relationships from other fluorinated hydrocarbon reactions, by *ab initio* transition state calculations, and by application of RRKM and QRRK methods. The chemistry was modeled by taking into consideration different flame configurations, including counterflow diffusion flames, methane and ethylene fuels, and various degrees of dopant concentration.

RESULTS and DISCUSSION

In Fig. 1, maximum temperature in the flame is plotted against the maximum oxidizer-side strain rate for different amounts of CHF_3 added to the oxidizer jet. Note that the addition of CHF_3 to the air jet has a two-fold effect on the flame structure: 1) it lowers the flame temperature for a fixed strain rate, and 2) it lowers the strain rate at which the flame extinguishes, i.e., the flame is more easily extinguished when CHF_3 is added to the oxidizer jet. Note, for example, that at a strain rate of 250 s^{-1} , one per cent CHF_3 lowers the maximum flame temperature by 19K, but that two per cent produces a flame much closer to extinction, lowering the maximum flame temperature by 50K. Clearly, a methane flame with three per cent CHF_3 added to the oxidizer jet cannot exist at a strain rate of 250 s^{-1} .

The full set of fluoromethanes, along with N_2 and CO_2 , are compared in Fig. 2 by their abilities (on a molar basis) to reduce the extinction strain rate in the counterflow methane vs. air flame. While none of the agents approach the flame-suppressing effectiveness of CF_3Br [8], CF_4 and CHF_3 are the two most effective C_1 fluorocarbon extinction agents, yielding nearly identical extinction results that improve nearly linearly with molar concentration. These results are in agreement with our earlier work on laminar flame speeds in doped, premixed, lean, freely propagating methane – air flames [3]. These species are followed in effectiveness by the diluent CO_2 . CH_2F_2 has the most ambiguous effect on the extinction characteristics of the counterflow methane vs. air diffusion flame, acting as a mild suppressant above concentrations of one mole per cent, and in fact, acting as a very mild flame enhancement agent at concentrations below one mole per cent. This result is in contrast to our earlier work on freely propagating flames, in which CH_2F_2 acted as a mild accelerant when added in any amount up to concentrations of three mole per cent, but is in agreement with the results of Linteris and Truett [4] for premixed methane-air flames. N_2 has effectiveness as a flame suppressant, its effect varying linearly with its concentration. CH_3F is the only C_1 additive which enhances the combustion (lowers the susceptibility to extinction) in the counterflow diffusion flame.

Calculations were performed for CHF_3 addition of up to eight mole per cent, to establish that this is nearly the highest doping under which a flame may exist. In other words, methane vs. air counterflow diffusion flames cannot exist with more than eight mole per cent CHF_3 added to the air stream, regardless of how little the flame is strained. The effectiveness of CF_4 appears diminished at higher loadings, and an extrapolation shows that low strain flames can exist slightly above CF_4 loadings of eight mole per cent. Since most fires would exist under low strain conditions, the difference in effectiveness between

CF_4 and CHF_3 at high loadings is significant.

The calculated flame suppression effectiveness of CF_4 and CHF_3 is compared against the extinction experiments of Papas et al. [8] in Fig. 3. (It should be noted that neither CF_4 nor CHF_3 caused sooting conditions in the experiments [16], in contrast to the soot formation observed in CF_3Br -suppressed flames. In fact, addition of CHF_3 has been observed to *reduce* soot levels in certain sooting flames [17].) Both computations and experiments show similar linear decreases in required extinction strain rate with molar per cent agent added to the oxidizer stream, with the calculations yielding a mildly steeper improvement. The experiments tend to mimic the diminished effectiveness of CF_4 at the higher loadings, although the effect is more pronounced in the calculations. The major discrepancy between the experiments and the calculations is that the model and associated chemical kinetic mechanism and thermodynamic data base predict moderately lower extinction strain rates throughout the entire range of suppressant addition level, *including* the unsuppressed flame. Thus, while the experimental decrease in extinction strain rate with increased suppressant loading is accurately predicted by the chemical mechanism, it appears that more of a discrepancy may exist with the *hydrocarbon* (H/C/O) portion of the kinetic mechanism, derived from [18], rather than with the fluorinated species.

Thus, the calculations for CHF_3 were rerun with two alternate sets of hydrocarbon kinetics — a compilation of earlier studies [19–22] which has been used, successfully, in determining the structure of two-dimensional axisymmetric laminar diffusion flames [23] (“alt. kin. 1”), and GRI-Mech version 2.11 [24] (“alt. kin. 2”). These hydrocarbon kinetics replaced the hydrocarbon portion of the present mechanism, with the fluorinated portion of the mechanism remaining intact. The results from these calculations are contrasted with the previous calculations in Fig. 4. Note that both alternate hydrocarbon mechanisms predict *higher* extinction strain rates for the unsuppressed flame, with GRI-Mech significantly overpredicting the experimental extinction strain rate. Interestingly, as the CHF_3 loading is increased, calculations from both alternate mechanisms approach those from the original mechanism. Thus, while the present mechanism seems to be the most reasonable choice for the present application, discrepancies between models and experiments throughout the range of suppressant loading may be traced to the hydrocarbon chemistry as well as the interaction between the hydrocarbon chemistry and the fluorine chemistry.

The effect of the C_2 fluorinated additives on flame suppression is illustrated in Fig. 5; results for CHF_3 are included for comparison. Both $\text{CHF}_2\text{-CF}_3$ and $\text{CH}_2\text{F-CF}_3$ appear to outperform all of the C_1 additives in flame suppression, when reckoned on a molar basis.

However, many applications of fire suppression agents are governed by storage and weight constraints — airborne applications, for instance. Thus, in practice, an analysis of suppressant effectiveness on a per mass basis may be more appropriate than the molar basis presented above. The simulations from Figs. 2 and 3, for the most effective suppression agents, are replotted on a per-mass basis in Fig. 6. Interestingly, the inerts N_2 and CO_2 seem to outperform moderately all of the fluorinated species, including CF_4 , CHF_3 and the C_2 species, on this basis. This is an important result, which may lessen the attractiveness of FCs and HFCs as replacements for halons 1301 and 1211 in certain applications.

We focus the remainder of the discussion on analyzing the modes of fire suppression taken by each additive. Some of the additives may act, simply, as high-heat-capacity diluents, while other may possess a chemical suppression component. In order to distinguish the physical from the chemical modes of suppression, we recalculated the extinction strain rates by first “turning-off” all of the fluorine chemistry in the kinetic mechanism. The results appear in Fig. 7. (Results are not presented for CF_4 since it is chemically inactive, for the most part.) Clearly, CHF_3 exhibits a chemical component of its suppression abil-

ity, as it yields higher extinction strain rates (particularly at the higher loadings) when its chemistry is turned-off. The apparent increase in the fraction of chemical contribution to suppression at increased CHF₃ loading is consistent with the numerical results of Noto et al. [5] for suppression of laminar flame speeds. Interestingly, calculated flame temperatures were observed to decrease more when the CHF₃ flame chemistry was turned-off, than compared to the decreases presented earlier in Fig. 1. This indicates that temperature increases, taken alone, do not *always* lead to increased flame stability. In contrast to CHF₃, the C₂ fluorinated hydrocarbons exhibit very little net chemical effect on extinguishing the counterflow flames, with somewhat ambiguous results throughout the range of suppressant loading.

Finally, we highlight some differences in chemical activity between the three fluorinated methane flame suppressants. Table 1 compares the maximum temperatures and peak HF and CF₂O concentrations between methane vs. air counterflow diffusion flames, all at the same strain rate of 183 s⁻¹ but differing in the particular additive in the air stream. (Each additive is at a concentration of four mole per cent.) The base case represents the counterflow diffusion flame with no additive. Addition of N₂ lowers the maximum temperature 57 K below the base case value. Addition of CF₄, which is mostly chemically inactive based on its small associated HF and CF₂O values, causes the flame temperature to drop by 173 K. The relative effectiveness of CF₄ over N₂ on a molar basis is approximately equal to the ratio of the additives' heat capacities. In contrast, CHF₃ is chemically active — 48 % of the fluorine atoms contribute to the peak value of HF, while another 37 % contribute to the CF₂O maximum concentration. On a strictly heat-capacity basis, the CHF₃ should have reduced the temperature to 1810 K. Since the temperature only dropped to 1875 K, we repeat the indication that the chemical activity of the CHF₃ tends to *raise* the combustion temperature. A similar argument may be made for CH₂F₂. These results are in accord with our earlier findings in freely propagating flames: CHF₃ suppressed flame speed despite raising the adiabatic flame temperature, and CH₂F₂ mildly enhanced flame speed while having a rather large effect on increasing the adiabatic flame temperature.

The main chemical difference between the action of CHF₃ and the action of CH₂F₂ is shown in [3]. Chemical pathways from CF₃ (formed from CHF₃) steer mainly to CF₂O, somewhat of a “dead end” kinetically because it is only slowly destroyed. In contrast, CHF₂ (from CH₂F₂) still has a labile hydrogen, opening faster routes to highly exothermic HF and CO₂ formation. Thus, heat is released more rapidly as CH₂F₂ is oxidized. The large portion of fluorine atom (up to 37%) originating in CHF₃ and bound-up in CF₂O is contrasted in Table 1 against the small (3%) amount of fluorine atom originating in CH₂F₂ which contributes to CF₂O formation.

CONCLUSIONS

A recently developed set of thermochemical and chemical kinetic data for the C₁ and C₂ fluorinated hydrocarbons has been used in the numerical investigation of the suppression properties of a variety of candidates selected for halon 1301 and halon 1211 replacement. On a molar basis, the C₂ fluorocarbons CHF₂-CHF₃ and CH₂F-CF₃ were the most effective agents in causing methane vs. air counterflow flames to extinguish. CF₄ and CHF₃ were the most effective C₁ suppression agents, with ability to extinguish flames comparable to each other, except at the highest loadings where the effectiveness of CHF₃ is enhanced by its chemical activity. On a mass basis, however, the inerts N₂ and CO₂ were comparable to or outperformed *all* of the fluorinated species in extinguishing the methane vs. air counterflow diffusion flames. This important result may lessen the attractiveness of fluorocarbons and hydrofluorocarbons in certain applications as replacements for halons 1301 and 1211.

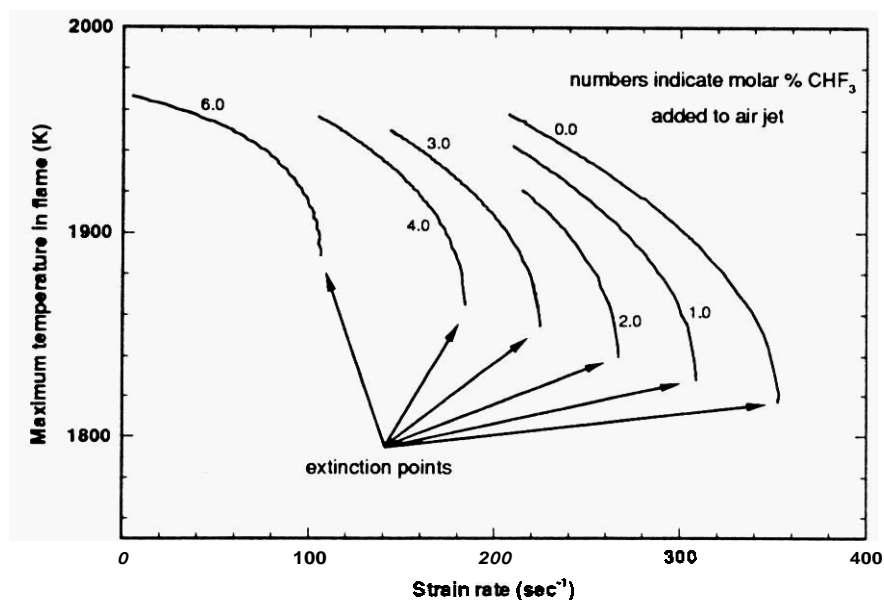
The chemical activity of CHF_3 was shown to contribute towards flame suppression, particularly at higher concentrations. In contrast, the C_2 hydrofluorocarbons appear to provide very little net chemical contribution towards extinguishing the counterflow diffusion flames, and in fact, may contribute to slight flame enhancement in some cases. Thus, their flame suppression activities stem primarily from their roles as high heat capacity diluents. Additives which lead to CF_2O formation are more effective flame suppression agents than those whose chemistry tends to bypass this pathway, as the relatively stable CF_2O molecule prevents certain amounts of C, F and O atoms from participating in highly exothermic CO_2 and HF formation.

REFERENCES

1. Zurer, P.S., *Chem. Eng. News*, 71 (46):12-18 (1993).
2. Grosshandler, W.L., Gann, R.G., "Low Environmental Impact Fire Suppression Concepts," invited presentation at the 1994 Fall Technical Meeting of the Eastern States Section of the Combustion Institute December 5-7, 1994, Clearwater Beach, FL, and appearing in **Chemical and Physical Processes In Combustion**, The Combustion Institute, Pittsburgh, 1994, p. 37.
3. Westmoreland, P.R., Burgess, Jr., D.R.F., Zachariah, M.R., Tsang, W., **Twenty-fifth Symposium (International) on Combustion**, The Combustion Institute, Pittsburgh, 1994, pp. 1505-1511.
4. Linteris, G.T., Truett, L., *Combust. Flame*, 105:15-27 (1996).
5. Noto, T., Babushok, V., Burgess, Jr., D.R., Hamins, A., Tsang, W., Miziolek, A., **Twenty-sixth Symposium (International) on Combustion**, The Combustion Institute, Pittsburgh, 1996, pp. 1377-1383.
6. Hamins, A., Trees, D., Seshadri, K., Chelliah, H.K., *Combust. Flame*, 99:221-230 (1994).
7. Fallon, G.S., Chelliah, H.K., Linteris, G.T., **Twenty-sixth Symposium (International) on Combustion**, The Combustion Institute, Pittsburgh, 1996, pp. 1395-1403.
8. Papas, P., Fleming, J.W., Sheinson, R.S., **Twenty-sixth Symposium (International) on Combustion**, The Combustion Institute, Pittsburgh, 1996, pp. 1405-1411.
9. Burgess, Jr., D.R.F., Zachariah, M.R., Tsang, W., Westmoreland, P.R., "Thermochemical and Chemical Kinetic Data for Fluorinated Hydrocarbons," NIST Technical Note 1412, U.S. Government Printing Office, Washington, D.C., July 1995 (and to appear in *Prog. Energy Combust. Sci.*).
10. Smooke, M.D., Crump, J., Seshadri, K., Giovangigli, V., **Twenty-third Symposium (International) on Combustion**, The Combustion Institute, Pittsburgh, 1990, pp. 463-470.
11. Chelliah, H.K., Law, C.K., Ueda, T., Smooke, M.D., Williams, F.A., **Twenty-third Symposium (International) on Combustion**, The Combustion Institute, Pittsburgh, 1990, pp. 503-511.
12. Giovangigli, V., Smooke, M.D., *Appl. Num. Math.* 5:305-331 (1989).
13. Giovangigli, V. and Darabiha, N., "Vector Computers and Complex Chemistry Combustion" in **Proceedings of the Conference on Mathematical Modeling in Combustion**, Lyon, France, NATO ASI Series, 1987.
14. Zachariah, M.R., Westmoreland, P.R., Burgess, Jr., D.R.F., Tsang, W., Melius, C.F., "BAC-MP4 Predictions of Thermochemical Data for C_1 and C_2 Stable and Radical Hydrofluorocarbons and Oxidized Hydrofluorocarbons," to appear in the *Journal of Physical Chemistry* (1996).
15. Zachariah, M.R., Tsang, W., Westmoreland, P.R., Burgess, Jr., D.R.F., *J. Phys. Chem.* 99:12512-12519 (1995).
16. Tanoff, M., Smooke, M., Papas, P., Fleming, J.W., Sheinson, R.S., **Twenty-sixth Symposium (International) on Combustion**, The Combustion Institute, Pittsburgh, 1996, p. 1411.

17. VanDerWege, B.A., Bush, M.T., Hochgreb, S., Linteris, G.T., "Effect of CF_3H and CF_3Br on Laminar Diffusion Flames in Normal and Microgravity," Eastern States Section of the Combustion Institute 1996 Fall Technical Meeting, Worcester, MA, October 16-18, 1995, and appearing in *Chemical and Physical Processes in Combustion*, The Combustion Institute, Pittsburgh, 1995.
18. Miller, J.A., Bowman, C.T., *Prog. Energy Comb. Sci.*, 15:287- (1989)
19. Warnatz, J., *Combust. Sci. and Tech.* 34:177-200 (1983)
20. Westbrook, C.K., Dryer, F.L., *Prog. Energy Comb. Sci.* 10:1-57 (1984).
21. Miller, J.A., Kee, R.J., Smooke, M.D., Grcar, J.F., "The computation of the structure and extinction limit of a methane-air stagnation point diffusion flame," Paper # WSS/CI84-10, 1984 Spring Meeting of the Western States Section of the Combustion Institute, Boulder, CO, April 2-3, 1984.
22. Norton, T.S., Smyth, K.C., *Combust. Sci. and Tech.* 76:1-20 (1991)
23. Smooke, M.D., Xu, Y., Zurn, R.M., Lin, P., Frank, J.H., Long, M.B., *Twenty-fourth Symposium (International) on Combustion*, The Combustion Institute, Pittsburgh, 1992, pp. 813-821.
24. Bowman, C.T., Hanson, R.K., Davidson, D.F., Gardiner Jr., W.C., Lissianski, V., Smith, G.P., Golden, D.M., Frenklach, M., Wang, H., Goldenberg, M., GRI-Mech version 2.11, <http://www.gri.org>, (1995).

FIGURE 1 — Calculated maximum temperature vs. maximum oxidizer-side strain rate in methane vs. air counterflow diffusion flames in which the air jet has been doped with varying amounts of CHF_3 . All curves terminate at the strain rate at which the flame extinguishes.



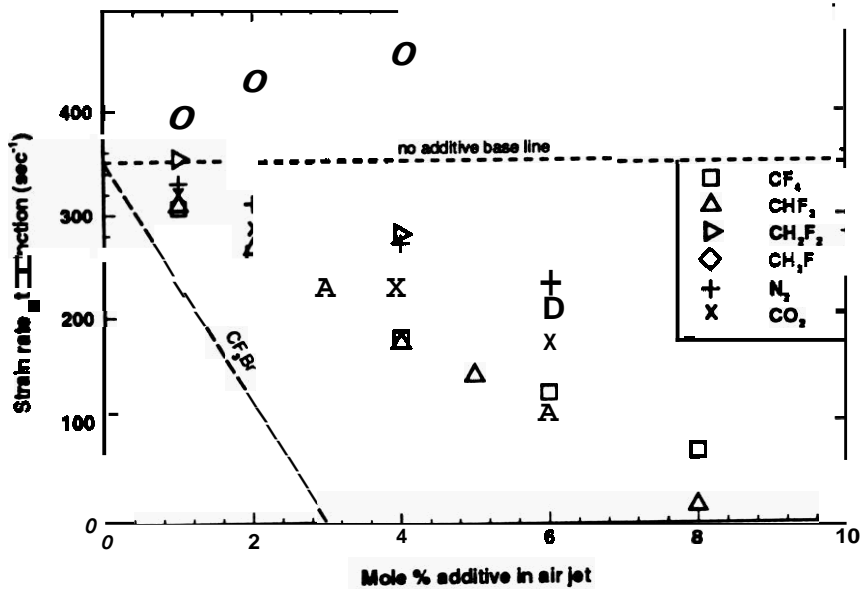


FIGURE 3 — Calculated extinction strain rate vs. mole per cent CF_4 or CHF_3 suppressant (hollow symbols), compared against the extinction measurements of Papas et al. [E] (solid symbols).

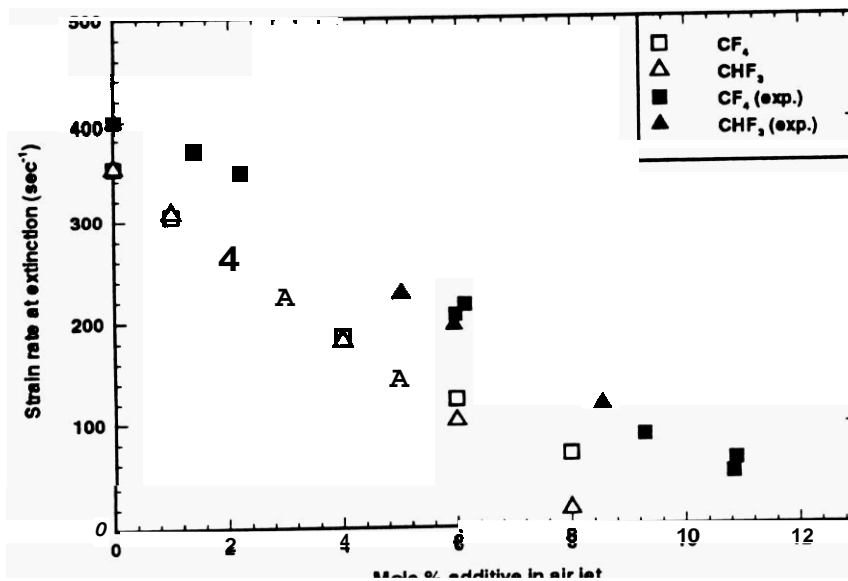


FIGURE 4 — Calculated extinction strain rate vs. mole per cent CHF_3 using three different kinetic mechanisms, as described in the text. "alt. kin. 1" uses H/C/O kinetics from prior compilations [19–22], and "alt. kin. 2" uses H/C/O kinetics from GRI-Mech 2.11 [24].

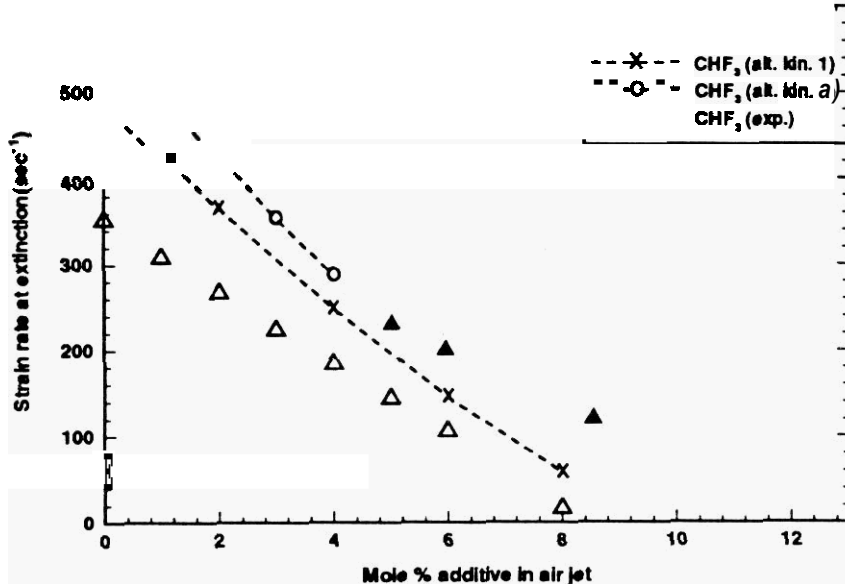


FIGURE 5 — Calculated extinction strain rate vs. mole per cent $\text{CHF}_2\text{-CHF}_3$ or $\text{CH}_2\text{F-CF}_3$ suppressant (solid symbols), compared against the suppression effectiveness of CHF_3 (hollow triangles).

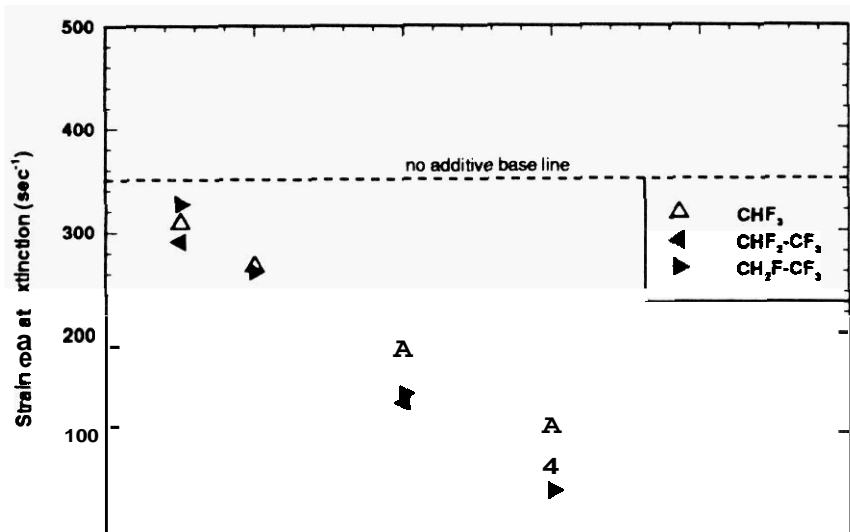


FIGURE 6 — Calculated extinction strain rate vs. *mass* per cent suppressant in the air jet of a methane vs. air counterflow diffusion flame.

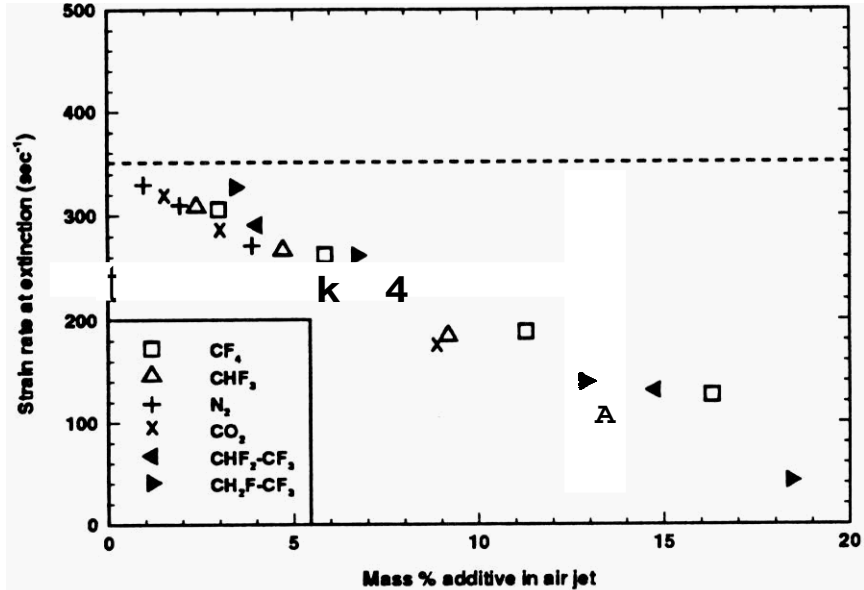


FIGURE 7 — Calculated extinction strain rate vs. mole per cent suppressant with fluorine chemistry "turned on" (hollow symbols) and "turned off" (solid symbols). Suppression effectiveness for N₂ is included for comparison.

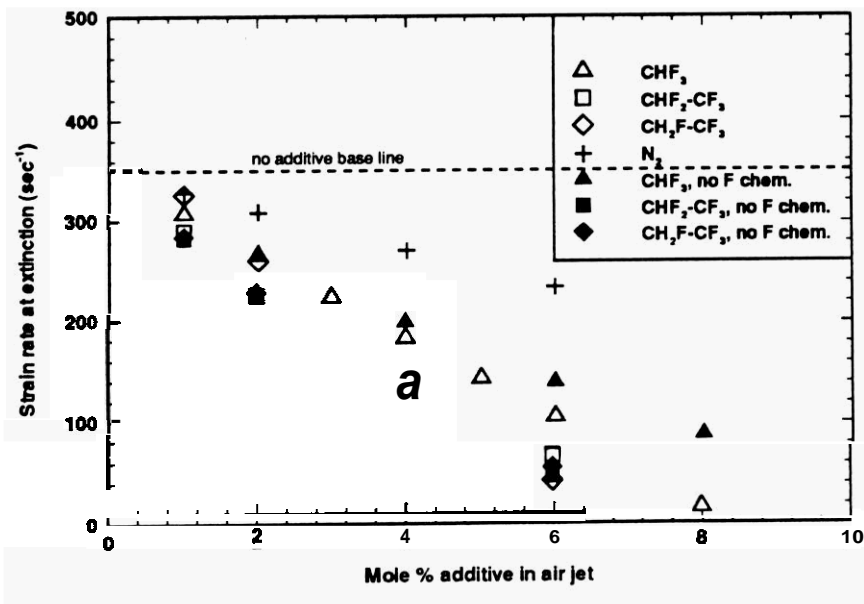


Table 1

A comparison of maximum flame temperatures and peak HF and CF₂O concentrations in methane vs. air counterflow flames, all at a strain rate of 183 s⁻¹, but differing in the suppressant added to the air stream. All suppressants are added at a concentration of four mole per cent.

Additive	$c_p \left(\frac{\text{Gal}}{\text{mol} \cdot \text{K}} \right)$	T_{max} (K)	[HF] _{max}	[CF ₂ O] _{max}
Base Case	—	1969	—	—
N ₂	7.8	1912	—	—
CF ₄	23.6	1796	1.1E-03	1.4E-04
CHF ₃	21.8	1875	5.8E-02	2.23E-02
CH ₂ F ₂	20.0	1989	6.3E-02	2.6E-03
